Hindawi
Journal of Food Quality
Volume 2022, Article ID 4412324, 11 pages
https://doi.org/10.1155/2022/4412324

Research Article

Effect of Different Polymerized Xylooligosaccharides on the Metabolic Pathway in *Bifidobacterium adolescentis*

Di Yao, Mengna Wu, Xiaoyu Wang, Lei Xu, and Xiqun Zheng

Department of Food Science and Engineering, College of Food, Heilongjiang Bayi Agricultural University, Daqing 163319, Heilongjiang Province, China

Correspondence should be addressed to Di Yao; yd13845991700@163.com

Received 29 November 2021; Accepted 9 February 2022; Published 7 March 2022

Academic Editor: Wen yi Kang

Metabolic pathway analysis of *Bifidobacterium adolescent* (*B. adolescentis*) grown on either xylobiose and xylotriose (X2/X3) or xylopentaose (X5) and identifying key regulatory-related genes and metabolites from RNA-seq and UHPLC system was performed. Compared with X5, X2/X3 highly promoted the growth of *B. adolescentis*. Also, the transcriptome analysis showed that a total of 268 differentially expressed genes (DEGs) of *B. adolescentis* cultured with X2/X3 and X5 were screened, including 163 upregulated and 105 downregulated genes (X2/X3 vs. X5), which mainly were ABC transporters. Furthermore, the qRT-PCR results of 16 DGEs validated the accuracy of the RNA-seq data. Meanwhile, metabolomics analysis showed that 192 differential metabolites noted on MS2 included 127 upregulated and 65 downregulated metabolites; mainly, metabolites were amino acids and organic acids. The abundance difference of specific genes and metabolites highlighted regulatory mechanisms involved in utilizing different polymerized xylooligosaccharides by *B. adolescentis*.

1. Introduction

Bifidobacterium is believed to play an important role in maintaining and promoting human health by eliciting a number of beneficial properties, such as improvement of gastrointestinal health [1] and immune function [2,3]. Bifidobacteria can utilize a diverse range of dietary carbohydrates that escape degradation in the upper parts of the intestine, many of which are plant-derived oligosaccharides [4–6]. Therefore, the plant-derived oligosaccharides can be used as a kind of prebiotics [7]. Accumulating evidence on probiotic and prebiotic interventions has demonstrated promising effects on promoting gastrointestinal health by modulating the microbiota toward the enrichment of beneficial microorganisms [8]. The effects of both probiotics and prebiotics on immune function have been well described in a range of studies including in vitro assessment studies, animal models, and human trials [2].

As a prebiotic candidate, xylooligosaccharides (XOS) have recently been shown to have promising effects on beneficial commensal microbes and health outcomes [3]. The most informative studies on XOS are those carried out by Okazaki et al. [9]. A volunteer trial involving feeding XOS to healthy humans showed significant increases in bifidobacteria. There was also a significant increase in the concentration of organic acids in the faeces. Additional studies have demonstrated that XOS stimulate the growth of caecal and faecal bifidobacteria at higher levels than the prebiotic fructooligosaccharide (FOS) [6,10]. Therefore, XOS have attracted more attention due to the highly selective proliferation effect on bifidobacteria.

Different bifidobacterial strains may possess different carbohydrate utilizing abilities. However, *B.adolescentis* is able to efficiently utilize XOS [11]. The genome of some species of bifidobacteria from humans and animal origin demonstrates a high presence of genes involved in the metabolism of complex oligosaccharides [12, 13]. Five gene clusters involved in the utilization of XOS have been identified [14]. In most cases, the genes encoding the transporter components and the associated catabolic enzymes for carbohydrates within a range of degrees of polymerization, similar monosaccharide constituents, or

linkage are clustered in conserved modules and coregulated as single operons [15]. In addition, Crittenden suggested that bifidobacteria were able to utilize XOS but not xylan [16]. In fact, bifidobacteria are unable to grow on xylan, owing to the extracellular xylan-degrading activity, thereby allowing efficient uptake of the produced XOS by a dedicated ABC transporter encoded by bifidobacteria [17]. Based on the XOS catabolic pathway, XOS (DP of 2 to 6) transported via the ABC system were hydrolyzed by endo-1,4-β-xylanases and β-xylosidases [18].

Although our previous studies have elucidated the utilization and metabolism of XOS in *B. adolescentis* 15703 and identified the key regulatory-related genes and metabolites. However, to date, no work has been carried out on the regulatory mechanisms that control the expression of the genes and metabolites involved in the metabolic pathways on different polymerized XOS. To address this issue, we performed combined transcriptome and metabolome analyses to elucidate the molecular mechanism for utilization and metabolism of different polymerized XOS in *B. adolescentis*.

2. Materials and Methods

2.1. Separation and Preparation of Different Polymerized XOS. Sephadex G-10 (Sigma, Saint Louis, MO, USA) was selected as a separation medium using preparative chromatography technology; xylobiose, xylotriose mixture (X2/X3), and xylopentaose (X5) from XOS were separated. The sample loading was 2 mL, the elution flow rate was 1.0 mL/min, and the injection concentration was 30%. On the basis of ensuring purity, X2/X3 and X5 were prepared using continuous preparative chromatography equipment and then were analyzed by HPLC. Chromatographic conditions were as follows: SUGAR KS-802 column, ultrapure water as mobile phase, the flow rate of 0.6 mL/min, and column temperature of 81 ˚C.

2.2. Cultivation of B. adolescentis 15703. B. adolescentis 15703 (General Microbiological Culture Collection Center, Beijing, China) was resuscitated and precultivated twice using MRS Broth (Hope Bio, China). Then, cells were harvested and suspended as 2% inoculation into an MRS medium containing X2/X3 or X5 and a control medium without carbohydrate and incubated at 37˚C under anaerobic conditions [19]. Cell growth was determined by measuring the optical density at 600 nm (OD600).

2.3. RNA-Seq Analysis. Cell pellets of *B. adolescentis* 15703 were harvested by centrifugation. The cells were used for extracting total RNA following the manufacturer's recommendations of the QIAGEN 74524 kit. After the concentration and purity of extracted RNA were qualified, the mRNA was enriched by removing rRNA using Ribo-Zero^{TM} Magnetic Kit (Epicentre). The mRNA was reverse-transcripted into cDNA; then, second strands were synthesized using DNA polymerase I, RNase H, and dNTP. The obtained cDNA fragments were purified, end-repaired, poly(A)-added, and ligated to Illumina sequencing adapters [19]. The ligation products size were chosen, amplified, and sequenced using Illumina HiSeq^{TM} 2500. The sequenced reads were mapped to a reference genome by TopHat2; then, the transcripts were merged from multiple groups into a finally comprehensive set of transcripts for further downstream differential expression analysis. Gene abundance was quantified by the RSEM software. The gene expression level was normalized with the FPKM method and the edgeR package was used to identify DEGs across groups. In comparison to significant DEGs, FDR <0.01 and Fold Change (FC) ≥ 2 were used as screening criteria. DEGs between X2/X3 and X5 treatments were conducted using the DEseq package. DEGs were subjected to enrichment analysis of KEGG pathways.

2.4. Quantitative Real-Time PCR. Total RNA was isolated as described above. Then the cDNA synthesis was performed using reverse transcriptase. The primers sequence are listed in Supplementary Table 1 and each reaction (20 μL mixture) contained 2 μL cDNA, 10 μL 2× SYBR Green qPCR Master Mix, 0.5 μL the forward and reverse primers, and 7.0 μL ddH2O. All qRT-PCR analyses were performed in ABI StepOnePlus and performed in two steps: first, predenaturation for 3 min and 45 cycles of denaturation for 3 s at 95, then annealing/extension for 30 s at 58˚C. Gene expression was normalized by the 2-ΔΔCt method, and the 16S rRNA gene was used as the normalized standard [20].

2.5. Metabolites' Extraction. The sample of 100 μL was accurately removed and placed in an EP tube, 300 μL methanol was added to start extraction, and 20 μL of internal standard substances was added, followed by vortex for 30 s. Then, the mixture tube was immersed into the ultrasonic bath with ice water and ultrasonically incubated in ice water for 10 min and incubated for 1 h at −20˚C to precipitate proteins. Then the mixture was centrifuged at 13000 rpm for 15 min at 4˚C. Moreover, 200 μL of the supernatant sample was transferred to a fresh 2 mL LC/MS glass vial, 20 μL from the supernatant of each sample was marked as QC samples, and another supernatant was used for the UHPLC-QTOF-MS analysis. All experiments were carried out in triplicate.

2.6. Metabolites' Analysis by LC-MS/MS. The UHPLC system (1290, Agilent Technologies) with a UPLC BEH Amide column (1.7 μm 2.1 $*$ 100 mm, Waters) coupled with Triple TOF 5600 (Q-TOF, AB Sciex) was used for LC-MS/MS analyses. Then, 25 mM NH4OAc and 25 mM NH4OH in water (pH = 9.75) (A) and acetonitrile (B) were used as the mobile phase. The elution gradient was as follows: 0 min, 95% B; 7 min, 65% B; 9 min, 40% B; 9.1 min, 95% B; 12 min, 95% B. The flow rate of the mobile phase was 0.5 mL min-1. The injection volume of the analytical solution was 3 μL. The Triple-TOF-MS was used for its ability to acquire MS/MS spectra on an information-dependent basis (IDA) during an LC/MS experiment. In this mode, the full scan survey MS data collect and trigger the acquisition of MS/MS spectra

depending on preselected criteria surveyed by the acquisition software (Analyst TF 1.7, AB Sciex) [21]. In each cycle, 12 precursor ions with intensity greater than 100 were chosen for fragmentation at collision energy (CE) of 30 V (15 MS/MS events with product ion accumulation time of 50 msec each). ESI source conditions were set as follows: ion source gas 1, 60 Psi; ion source gas 2, 60 Psi; curtain gas, 35 Psi; source temperature, 650°C; ion spray voltage floating (ISVF), 5000 V or -4000 V in positive or negative modes, respectively.

The mzXML format was obtained using ProteoWizard to convert MS raw data files and processed by *R* package XCMS (version 3.2). The processed results generated a data matrix consisting of retention time (RT), mass-to-charge ratio (m/*z*) values, and peak intensity. *R* package CAMERA was used for peak annotation after XCMS data processing [22]. The metabolites were identified by the in-house MS_2 database.

3. Results and Discussion

3.1. Growth Characteristics of B. adolescentis on X2/X3 and X5. The HPLC analysis of the prepared X2/X3 and X5 was shown in Supplementary Figure 1. According to the results of the composition analysis, the purity of X2/X3 and X5 was 87.29% and 90.05%, respectively. Then, the X2/X3 and X5 were used as a carbon source to cultivate *B. adolescentis*. As shown in Figure 1, the growth of *B. adolescentis* on different polymerized XOS was significantly higher than that of the blank control group without a carbon source. The OD value of cultures of *B. adolescentis* with X2/X3 as the carbon source is the highest, X5 is the second, and xylose is the lowest; however, the lag and logarithmic phase is the shortest. Also, a rapid growth rate was observed at 8–20 h. The growth yield (stable phase) on X2/X3 was about 1.3-fold greater than that on X5, indicating that XOS at a lower degree of polymerization was more preferred by *B. adolescentis*. *Bifidobacterium* can preferentially hydrolyze XOS with a low degree of polymerization and then use monosaccharides for further metabolism. This result is consistent with the conclusion reported by Okazaki that oligosaccharides are more easily absorbed and utilized by bifidobacteria than by polysaccharides and corresponding monosaccharides [9]. The composition of X2 and X3 is entirely composed of xylose units and does not contain arabinosyl groups and substituents such as methoxy and acetyl groups, while X5 often contains arabinosyl isomers, which should firstly be degraded by arabinosidase [23]; this higher complexity may lead to a significant difference in the proliferation effect of X2/X3 and X5 on *B. adolescentis*.

3.2. Annotation and Analysis of Differentially Expressed Genes (DEGs) of B. adolescentis on X2/X3 and X5. A total of 268 DEGs were identified for *B. adolescentis* grown on X2/X3 and X5, including 163 upregulated genes and 105 downregulated genes (Supplementary Figure 2). The DEGs involved in biological functions were further analyzed by KEGG, and 20 pathways were predicted (Figure 2). ABC transporters, starch and sucrose metabolism, pyrimidine metabolism, and galactose metabolism are the highly represented categories. Among these pathways, the QValue of ABC transporters is the lowest (red color), suggesting the different encoding genes of ABC transporters is the most.

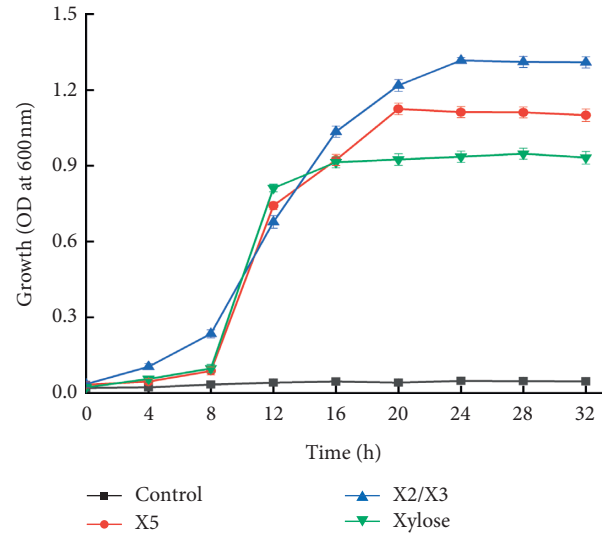

Figure 1: Growth of *B. adolescentis* on different polymerized XOS and control medium (no carbohydrate).

The DEGs involved in the ABC transporters are shown in Table 1. In the ABC transporter pathway, 33 genes were significantly upregulated. Genes BAD_RS00340 and BAD_RS07050 encoded ABC transporter. Genes BAD_RS01000, BAD_RS07410, BAD_RS02260, BAD_RS04685, BAD_RS00815, BAD_RS00810, BAD_RS08280, BAD_RS02545, BAD_RS06685, BAD_RS08205, BAD_RS08275, BAD_RS03705, BAD_RS06690, and BAD_RS08210 encoded ABC transporter permease. Genes BAD_RS02255, BAD_RS07415, BAD_RS01495, BAD_RS00805, BAD_RS00390, BAD_RS08285, BAD_RS08340, BAD_RS00990, and BAD_RS06680 encoded ABC transporter substrate-binding protein. Genes BAD_RS08285, BAD_RS00805, and BAD_RS02355 encoded solute-binding protein. Genes BAD_RS04090, BAD_RS00495, BAD_RS01005, BAD_RS03710, and BAD_RS00520 encoded ABC transporter ATP-binding protein. Five genes (BAD_RS02355, BAD_RS05605, BAD_RS03210, BAD_RS03215, and BAD_RS05655), which are ABC transporter-related genes, were significantly downregulated after X5 treatment.

The DEGs involved in carbohydrate metabolism are shown in Table 2. Compared to X2/X3 treatment, five genes (BAD_RS06400, BAD_RS07395, BAD_RS07400, BAD_RS08325, and BAD_RS08455) encoded beta-galactosidase and two genes (BAD_RS08195 and BAD_RS08270) encoded alpha-amylase related to starch and sucrose metabolism (ko00500), galactose metabolism pathway (ko00052), glycan degradation (ko00511), and sphingolipid metabolism (ko00600) were significantly upregulated after X5 treatment. The beta-xylosidase that encoded gene

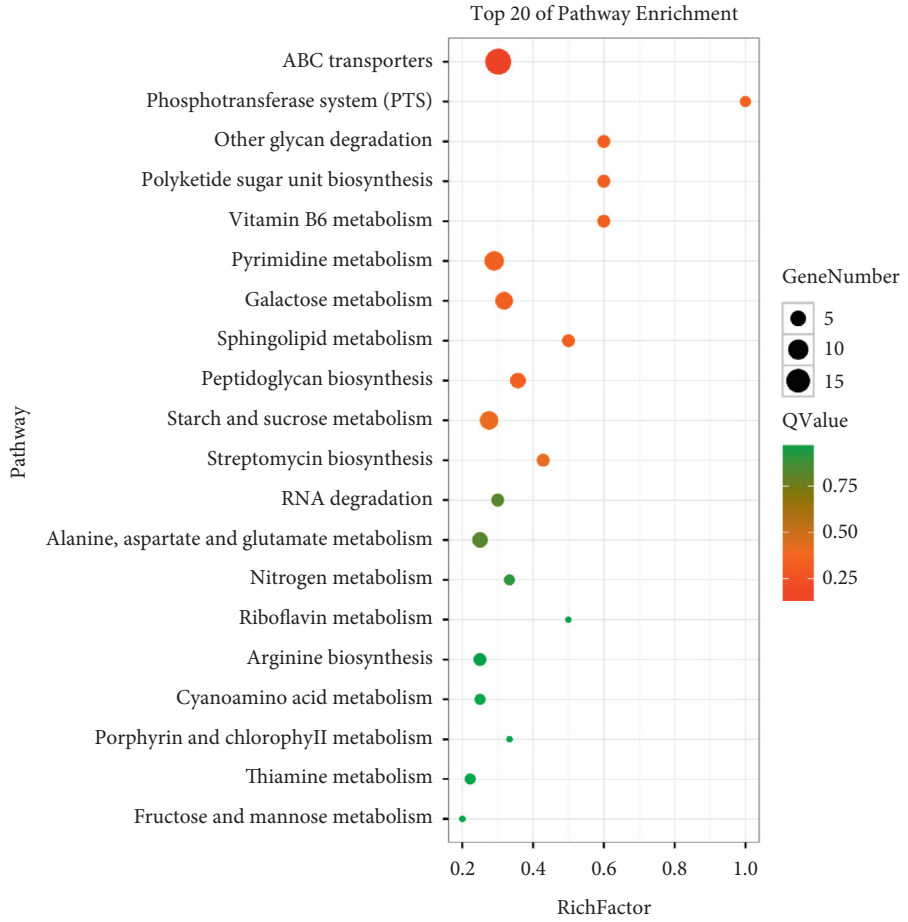

Figure 2: KEGG pathway enrichment analysis of DEGs (X2/X3 vs. X5). The vertical axis indicates the name of the KEGG pathway, and the horizontal axis indicates the rich factor. The dot size indicates the number of differentially expressed genes in the pathway, and the color of the dots corresponds to different Q values.

BAD_RS02270 was involved in amino sugar and nucleotide sugar metabolism (ko00520) and starch and sucrose metabolism (ko00500). Moreover, two genes (BAD_RS06365 and BAD_RS08480) encoded beta-glucosidase related to starch and sucrose metabolism (ko00500). Two genes (BAD_RS06360 and BAD_RS08405) encoded glycoside hydrolase involved in starch and sucrose metabolism (ko00500). In addition, gene BAD_RS01050 coded shikimate kinase, BAD_RS05480 coded mannan endo-1,4-beta-mannosidase, BAD_RS01040 coded 6-phosphogluconate dehydrogenase, BAD_RS02150 coded lactaldehyde reductase, BAD_RS07445 coded L-ribulose-5-phosphate 4-epimerase, BAD_RS01580 coded UDP-N-acetylenolpyruvoylglucosamine reductase, which was involved in the biosynthesis of antibiotics (ko01130), peptidoglycan biosynthesis (ko00550), microbial metabolism in diverse environments (ko01120), carbon metabolism (ko01200), fructose and mannose metabolism (ko00051), pentose phosphate pathway (ko00030), glyoxylate and dicarboxylate metabolism (ko00630), propanoate metabolism (ko00640), and pentose and glucuronate interconversions (ko00040), which was significantly upregulated after X5 treatment. Only one gene, BAD_RS07575, encoded alpha-1,4-glucan-maltose-1-phosphate maltosyltransferase, which was significantly downregulated after X5 treatment.

3.3. Validation of Transcript Abundance Using qRT-PCR. To verify the RNA-seq results, the mRNA expressions of 16 selected candidate genes (eight upregulated and eight downregulated) were measured by qRT-PCR. The normalized fold expressions of 16 DEGs are shown in Figure 3(a); the results showed that the upregulated and downregulated levels of these genes are consistent with RNA-seq. Furthermore, the expression levels of 16 DEGs with qRT-PCR were compared to those of DEGs with RNA-seq by the linear fitting. A significant correlation ($R2 = 0.98642$) was found between RNA-seq and qRT-PCR (Figure 3(b)). The qRT-PCR results are consistent with their transcript abundance in RNA-seq, which verified the accuracy of the DEGs from RNA-seq analyses.

3.4. Metabolite Profile and KEGG Mapping of Metabolites. The metabolites profiling of *B. adolescentis* was performed using LC-MS. The primary metabolites are amino acids, organic acids, fatty acids, polyhydroxy acids, sugars, polyols, and N-compounds. A total of 192 different metabolites (MS2) were identified for X2/X3 and X5 treatments ($p < 0.05$, log2FC > 1), including 127 upregulated metabolites and 65 downregulated metabolites. The different

Table 1: DEGs involved in the related ABC transporter during the growth of *B. adolescentis* on X5 compared to X2/X3 assessed by RNA-seq.

Gene no.[a]	Log_2 (Fc)[b]	*P* value	FDR	Symbol	Annotation[c]	Linear FMPK value[d]	
						X2/X3	X5
BAD_RS02255	3.01↑	0	0	yurO	Sugar ABC transporter substrate-binding protein	989.28	7940.17
BAD_RS07415	2.79↑	$4.47E-86$	$1.40E-84$	mdxE	ABC transporter, solute-binding protein	51.88	360.4
BAD_RS07410	2.75↑	$2.30E-19$	$1.78E-18$	amyD	ABC transporter permease	16.53	111.24
BAD_RS02265	2.57↑	0	0	yurM	Thiamine ABC transporter ATP-binding protein	514.59	3056.15
BAD_RS02260	2.57↑	0	0	malF	Sugar ABC transporter permease	466	2759.99
BAD_RS01495	2.51↑	$2.51E-261$	$2.23E-259$	TP_0034	ABC transporter substrate-binding protein	319.83	1819.21
BAD_RS00805	2.17↑	0	0	yurO	Solute-binding protein of ABC transporter system	618.73	2790.2
BAD_RS04685	1.87↑	0.0072	0.0164	-	ABC transporter permease	6.84	25.03
BAD_RS00385	1.75↑	0.0119	0.0254	livF	ABC-type branched-chain amino acid transport systems ATPase component	5.2	17.55
BAD_RS00390	1.74↑	0.0012	0.0031	BR1785	Branched-chain amino acid ABC transporter substrate-binding protein	6.05	20.15
BAD_RS00815	1.58↑	$3.35E-73$	$8.39E-72$	araQ	Sugar ABC transporter permease	326.41	974.92
BAD_RS07050	1.56↑	0	0	lipO	ABC transporter	3361.71	9912.7
BAD_RS00810	1.53↑	$2.70E-62$	$5.55E-61$	yurN	Sugar ABC transporter permease	278.86	804.48
BAD_RS08280	1.51↑	$3.55E-100$	$1.18E-98$	msmF	Sugar ABC transporter permease	491.14	1401.37
BAD_RS08285	1.51↑	$7.82E-193$	$4.82E-191$	ugpB	ABC transporter, solute-binding protein	686.94	1954.61
BAD_RS04090	1.51↑	0.0008	0.0022	TM_0352	Macrolide ABC transporter ATP-binding protein	15.42	43.86
BAD_RS00495	1.46↑	$1.94E-31$	$2.32E-30$	MT1311	Multidrug ABC transporter ATP-binding protein	81.69	225.1
BAD_RS01005	1.39↑	0.0242	0.0478	fbpC	ABC transporter ATP-binding protein	6.07	15.95
BAD_RS08340	1.36↑	$1.22E-07$	$4.99E-07$	msmE	Sugar ABC transporter substrate-binding protein	27.59	70.62
BAD_RS00990	1.31↑	0.0009	0.0024	-	ABC transporter substrate-binding protein	13.91	34.5
BAD_RS03710	1.30↑	$9.00E-05$	0.0002	lolD	ABC transporter ATP-binding protein	26.53	65.31
BAD_RS08210	1.27↑	$1.50E-107$	$5.58E-106$	amyD	Permease of ABC transporter possibly for oligosaccharides	933.34	2256.42
BAD_RS00520	1.27↑	$4.19E-18$	$3.02E-17$	Tpd	Amino acid ABC transporter substrate-binding protein	173.12	416.3
BAD_RS02545	1.25↑	0.0080	0.0178	gsiC	ABC transporter permease	11.65	27.77
BAD_RS03325	1.22↑	$2.33E-10$	$1.15E-09$	MJ1508	ABC transporter ATP-binding protein	85.46	198.92
BAD_RS06680	1.17↑	$2.10E-26$	$2.13E-25$	yxeM	Amino acid ABC transporter substrate-binding protein	228.62	513.46
BAD_RS06685	1.15↑	$3.29E-17$	$2.29E-16$	tcyL	ABC transporter permease	196.97	437.68
BAD_RS08205	1.15↑	$2.91E-56$	$5.54E-55$	amyC	Sugar ABC transporter permease	603.5	1334.63
BAD_RS08275	1.13↑	$1.22E-40$	$1.82E-39$	amyC	ABC transporter permease	413.73	903.85
BAD_RS03705	1.11↑	$5.91E-06$	$1.98E-05$	-	ABC transporter permease	35.95	77.6
BAD_RS00340	1.10↑	$1.30E-31$	$1.61E-30$	Pip	ABC transporter	109.76	235.38
BAD_RS06690	1.03↑	$2.25E-05$	$7.07E-05$	patM	ABC transporter permease	65.13	133.26
BAD_RS02355	1.35↓	$5.99E-14$	$3.50E-13$	braC	Solute-binding protein of ABC transporter for branched-chain amino acids	171.31	67.28
BAD_RS05605	1.53↓	$4.01E-12$	$2.20E-11$	-	Sugar ABC transporter substrate-binding protein	247.02	85.73
BAD_RS03210	2.07↓	$1.34E-44$	$2.10E-43$	lolD	Peptide ABC transporter ATP-binding protein	496.58	118.13
BAD_RS03215	2.76↓	$4.00E-186$	$2.37E-184$	macB	ABC transporter permease	480.91	71.17
BAD_RS05655	2.93↓	$8.53E-06$	$2.81E-05$	bceA	ABC transporter ATP-binding protein	31.99	4.2

[a]Gene number referenced as *B. adolescentis* being alphabet and a five-digit number. [b]Significance of fold change data is judged by having a *P* value of no more than 0.01. [c]Gene annotations were blasted against Swiss-Prot. [d]FPKM (fragments per kilobase of exon per million fragments mapped) values for cultures on media with X2/X3 or X5 treatment.

metabolites were annotated in 50 KEGG pathways. ABC transporters and the phosphotransferase system (PTS) were classified as environmental information processing. Aminoacyl-tRNA biosynthesis was included in genetic information processing. The remaining 47 pathways belong to metabolism processing, microbial metabolism in diverse environments, and biosynthesis of secondary metabolites, which are the most highly represented in metabolism processing (Figure 4).

Different metabolites involved in carbohydrate transport and metabolism are shown in Table 3. Compared to X2/X3 treatment, ten metabolites (meta_15, meta_376, meta_166, meta_1695, meta_651, meta_246, meta_219, meta_527, meta_82, and meta_991), which are glycerol, D-ribose, D-mannose, maltotriose, D-biotin, D-mannitol, L-arginine, L-cystine, L-isoleucine, and cellobiose, are significantly different in the ABC transporters pathway (ko02010) for X5 treatment. Also, eight metabolites, including D-mannose,

Table 2: DEGs involved in related carbohydrate metabolism in the KEGG pathway during the growth of *B. adolescentis* on X5 compared to X2/X3 assessed by RNA-seq.

Gene no.	Log_2 (Fc)	*p* value	FDR	Symbol	Annotation	Linear FMPK value		KEGG pathway
						X2/X3	X5	
BAD_RS06400	1.04↑	4.00*E* − 05	0.0001	bgaB	Beta-galactosidase	19.79	40.65	ko00052
BAD_RS07395	1.07↑	1.12*E* − 18	8.34*E* − 18	bgaB	Beta-galactosidase I	84.64	177.96	ko00052
BAD_RS07400	2.10↑	7.31*E* − 18	5.21*E* − 17	BGAL16	Beta-galactosidase	13.06	56.17	ko00052/ ko00600/ ko00511
BAD_RS08195	1.78↑	0	0	malL	Alpha-amylase	733.05	2512.17	ko00500/ ko00052
BAD_RS08270	1.36↑	1.8*E* − 148	9.3*E* − 147	malL	Alpha-amylase	493.04	1264.3	ko00500/ ko00052
BAD_RS08325	1.62↑	1.75*E* − 23	1.54*E* − 22	lacZ	Beta-galactosidase	25.2	77.45	ko00052/ ko00600/ ko00511
BAD_RS08455	1.04↑	3.10*E* − 35	4.07*E* − 34	lacZ	Beta-galactosidase	126.46	259.45	ko00052/ ko00600/ ko00511
BAD_RS02270	2.22↑	5.69*E* − 247	4.56*E* − 245	xynB	Beta-xylosidase	251.3	1174.15	ko01100/ ko00500/ ko00520
BAD_RS06360	1.08↑	2.76*E* − 56	5.32*E* − 55	xynB	Glycoside hydrolase 43 family protein	362.57	764.37	ko01100/ ko00500/ ko00520
BAD_RS06365	1.52↑	2.76*E* − 123	1.23*E* − 121	exgA	Beta-glucosidase	475.02	1358.67	ko00500
BAD_RS07575	1.18↓	1.84*E* − 112	7.20*E* − 111	glgE	Alpha-1,4-glucan--maltose-1-phosphate maltosyltransferase	1093.58	481.27	ko01100/ ko00500/
BAD_RS08405	1.03↑	4.88*E* − 06	1.64*E* − 05	bglB	Glycosyl hydrolase	21.72	44.24	ko01100/ ko01110/ ko00500/ ko00460
BAD_RS08480	1.11↑	2.43*E* − 18	1.79*E* − 17	bglB	Beta-glucosidase	66.25	142.54	ko01100/ ko01110/ ko00500/ ko00460
BAD_RS05480	1.31↑	4.84*E* − 08	2.04*E* − 07	BAD_1030	Mannan endo-1,4-beta-mannosidase	13.79	34.24	ko00051
BAD_RS01580	1.05↑	6.05*E* − 12	3.28*E* − 11	murB	UDP-N-acetylenolpyruvoylglucosamine reductase	93.71	194.42	ko01100/ ko00520/ ko00550
BAD_RS07445	1.38↑	5.29*E* − 30	6.09*E* − 29	ulaF	L-ribulose-5-phosphate 4-epimerase	229.09	594.72	ko01100/ ko00040
BAD_RS01040	2.09↑	6.41*E* − 24	5.84*E* − 23	Gnd	6-Phosphogluconate dehydrogenase	45.07	192.09	ko01100/ ko01110/ ko01130/ ko01120/ ko01200/ ko00480
BAD_RS01050	3.46↑	2.25*E* − 23	1.97*E* − 22	Idnk	Shikimate kinase	15.68	172.02	ko01100/ ko01110/ ko01130/ ko01120/ ko01200/ ko00030
BAD_RS02150	1.69↑	0	0	fucO	Lactaldehyde reductase	1795.21	5803.32	ko01120/ ko00630/ ko00640

cellobiose, D-mannitol-1-phosphate (meta_759), L-ascorbic acid (meta_312), D-sorbitol-6-phosphate (meta_761), N-acetyl-D-glucosamine-6-phosphate (meta_754), D-mannitol, and pyruvate (meta_8) are significantly different in the phosphotransferase system (PTS) (ko02060) for X5 compared to X2/X3 treatment. In addition, these

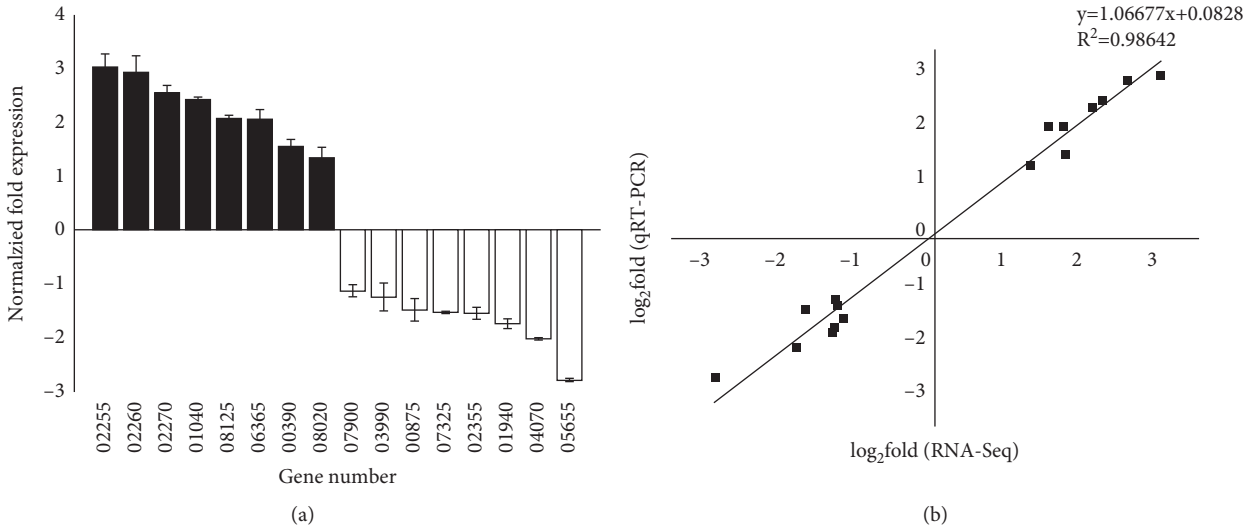

Figure 3: Results of expression profiles (a) and the linear fitting (b) of DEGs by qRT-PCR. Black column: upregulated; blank column: downregulated.

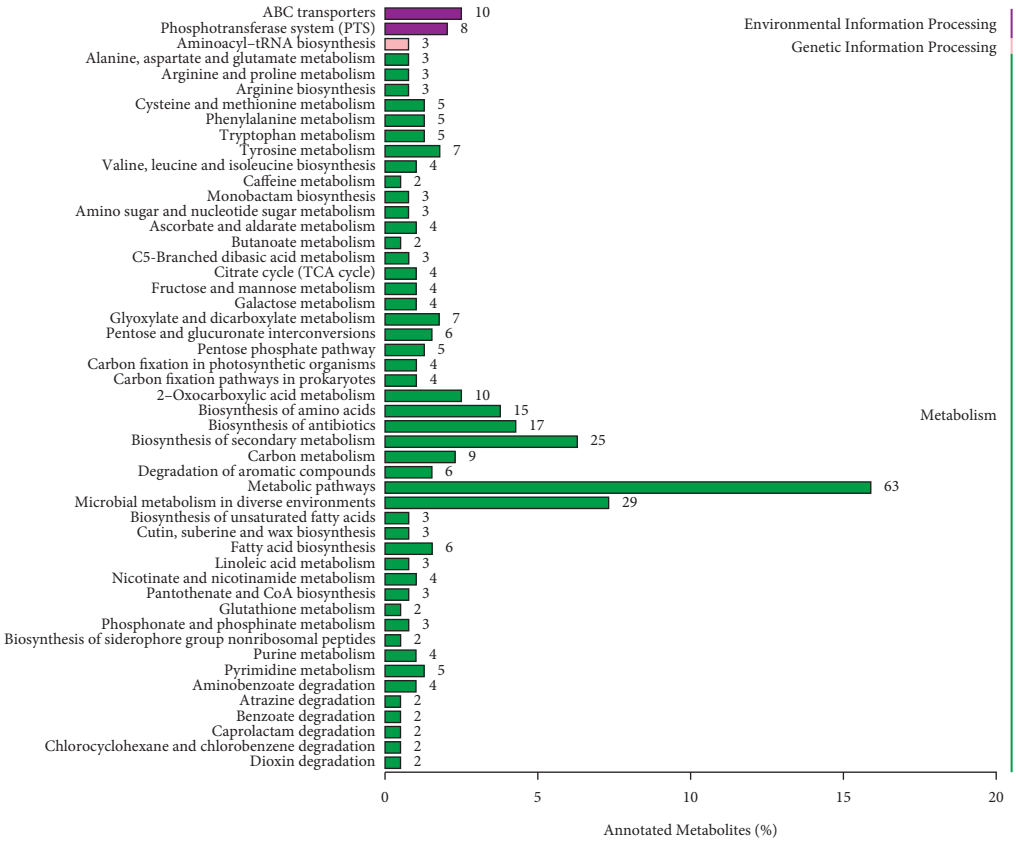

Figure 4: The annotated and classified results of the differential metabolite in the KEGG pathway.

metabolites, such as D-mannitol, D-mannose, D-mannitol-1-phosphate, and D-sorbitol-6-phosphate, were involved in fructose and mannose metabolism (ko00051). D-Ribose, pyruvate, and D-ribose-5-phosphate are involved in the pentose phosphate pathway (ko00030). However, galactinol, stachyose, and glycerol are involved in galactose metabolism (ko00052). Among all the metabolites, pyruvate (meta_8) is involved in most pathways, including pyruvate metabolism (ko00620), pantothenate and CoA biosynthesis (ko00770), glycolysis/gluconeogenesis (ko00010), and citrate cycle (ko00020).

Table 3: Metabolites involved in related carbohydrate transport and metabolism in the KEGG pathway during the growth of *B. adolescentis* on X5 compared to X2/X3 assessed by metabolome.

Meta ID	Log_2 (Fc)	MS2 name	mzmed	rtmed	KEGG_pathway_annotation
meta_15	1.591↑	Glycerol	91.042	107.553	ko00052/ko00040/ko02010/ko01100/ko00561
meta_376	2.919↓	D-Ribose	209.070	204.675	ko02010/ko00030/ko02030
meta_166	1.701↑	D-Mannose	161.048	418.573	ko00520/ko02060ko00052/ko00051/ko02010/ko01100
meta_1695	1.226↑	Maltotriose	563.190	430.279	ko02010
meta_651	1.260↑	D-Biotin	260.109	104.804	ko00780/ko02010/ko01100
meta_246	1.362↑	D-Mannitol	182.077	282.069	ko02010/ko00051/ko02060
meta_219	1.027↑	L-Arginine	173.106	380.973	ko00261/ko00970/ko01100/ko00472/ko01130/ko00331/ko00220/ko02010/ko01110/ko00330/ko01230/
meta_527	1.820↑	L-Cystine	239.020	413.417	ko02010/ko00270
meta_82	1.306↑	L-Isoleucine	130.089	221.442	ko02010/ko01230/ko00970/ko01130/ko00290/ko00280/ko00460/ko01210/ko01110
meta_991	1.647↑	Cellobiose	341.113	281.354	ko00500/ko02060/ko02010/ko01100
meta_759	1.072↑	D-Mannitol-1-phosphate	283.125	138.928	ko00051/ko02060
meta_312	4.861↓	L-Ascorbic acid	197.005	45.633	ko01100/ko01120/ko02060/ko00053/ko01110/ko00480
meta_761	4.397↑	D-Sorbitol-6-phosphate	283.128	44.744	ko02060/ko00051
meta_754	1.046↑	N-Acetyl-D-glucosamine 6-phosphate	282.034	128.662	ko01100/ko02060/ko01130/ko00520
meta_2004	2.193↑	Galactinol	683.235	370.331	ko00052
meta_2096	1.645↑	Stachyose	725.246	464.357	ko00052
meta_8	1.198↓	Pyruvate	87.011	54.515	ko00440/ko00760/ko00900/ko01220/ko00630/ko01120/ko00622/ko01210/ko00040/ko00620/ko00770/ko00362/ko01130/ko00270/ko00010/ko00020/ko01110/ko00250//ko01100/ko00730/ko00330/ko00290/ko02060/ko00680/ko01230/ko00360/ko01200/ko01502/ko00710/ko00720/ko00030
meta_1816	1.128↑	UDP-N-acetylglucosamine	606.0818147	409.813	ko00524/ko00520/ko00550/ko00540/ko01130/ko01502/ko01100
meta_29 3	1.293↓	Citrate	191.022	376.386	ko01130/ko01100/ko00720/ko01230/ko02020/ko00020/ko01110/ko01210/ko00250/ko01200/ko01120/ko00630
meta_211	2.899↑	Isocitrate	173.012	478.821	ko01230/ko01110/ko00020/ko01210/ko01200/ko01120/ko00630/ko01130/ko01100/ko00720
meta_365	1.042↑	Alpha-ketoglutarate	205.039	396.502	ko00720/ko01100/ko00053/ko00660/ko00430/ko00250/ko00365/ko00650/ko01200/ko00020/ko01110/ko01230/ko00340/ko00471/ko01130/ko01120/ko00220/ko00630/ko01210/ko00040/ko00300
meta_85	2.181↑	D-Xylulose	131.037	357.043	ko00040/ko01100
meta_130	1.709↓	D-Lyxose	149.049	301.108	ko00040
meta_135	3.108↑	Ribitol	151.064	232.243	ko00740/ko01100/ko00040
meta_1	1.551↓	Dihydroxyacetone	71.016	198.357	ko01100/ko01200/ko01120/ko00561/ko00680
meta_4	1.205↓	Glycolate	75.010	262.283	ko00361/ko01110/ko00625/ko01120/ko01200/ko00630/ko01130/ko01100
meta_74	1.033↓	Citraconic acid	129.022	73.135	ko00630/ko01200/ko01210/ko01100/ko00290/ko00660
meta_789	1.496↑	D-Ribose 5-phosphate	289.037	442.521	ko00440/ko01110/ko01230/ko01120/ko01200/ko00230/ko01130/ko00710/ko00030/ko01100

3.5. Effects of Specific Genes and Metabolites on XOS Transportation and Metabolism. Numerous carbohydrate uptake systems [24], especially ATP-binding cassette (ABC) importers, are encoded by bifidobacteria [25]. The affinity and specificity of ABC importers are defined largely by the extracellular solute-binding proteins (SBP) in bifidobacteria [26]. Compared to X2/X3, the gene expression of substrate-binding proteins (BAD_RS02255 and BAD_RS08340) and solute-binding proteins (BAD_RS07415, BAD_RS00805, and BAD_RS08285) was upregulated in the X5 treatment group, while one substrate-binding protein BAD_RS05605 was downregulated. The upregulation of binding protein indicates that XOS with higher polymerized degree indicated that required higher expression of binding proteins in *B. adolescentis* to better bind substrate. After the initial capture by SBPs, oligosaccharide ligands are released into the permease of the transporter, which is formed by two transmembrane domains (TMD), and the translocation is coupled to ATP-hydrolysis by cytoplasmic nucleotide-binding domains [27,28]. Compared with the X2/X3, the gene expression of ABC transporter permease (BAD_RS08280, BAD_RS02260, BAD_RS08210, BAD_RS08275, and BAD_RS08205) was upregulated in X5 treatment, while gene BAD_RS03215 was downregulated.

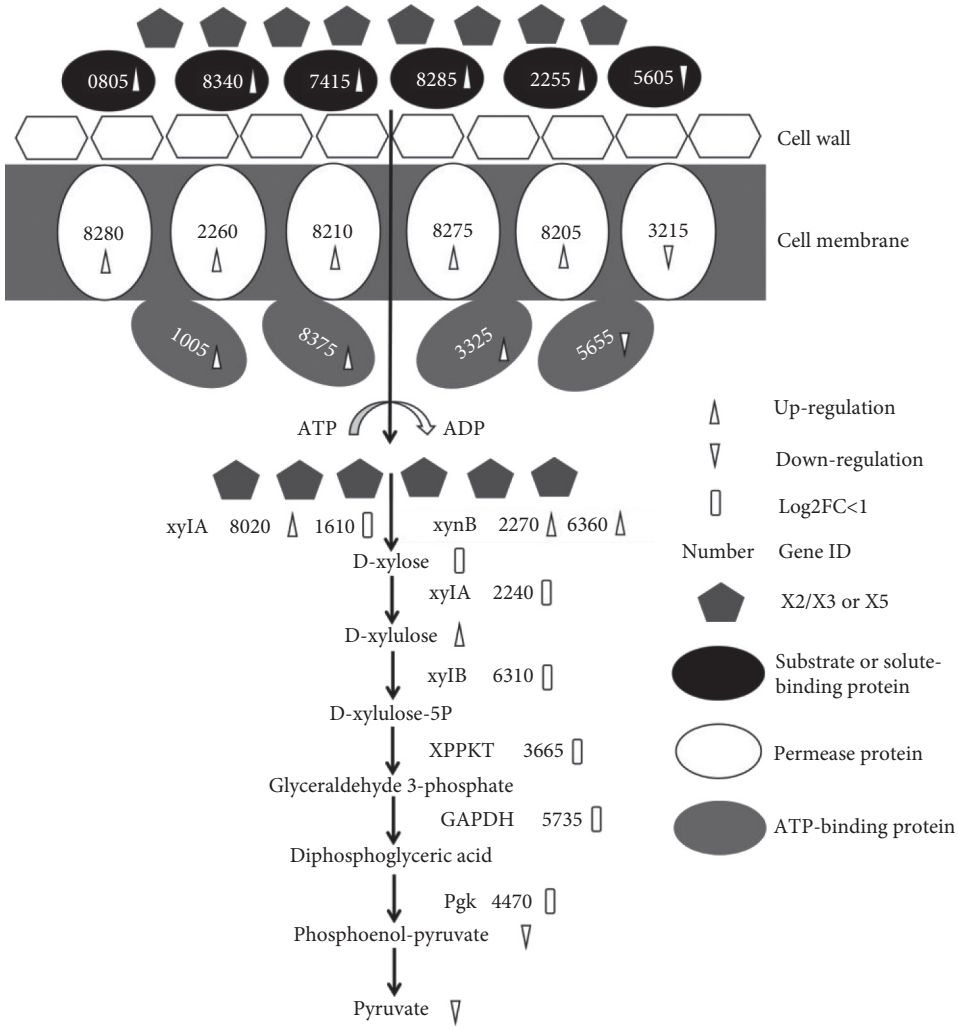

Figure 5: Proposed model for the catabolism of different polymerized XOS in *B. adolescents*. The numbers indicated the respective genes in the genome of *B. adolescents*, omitting the "BAD_RS."

Genes BAD_RS01005, BAD_RS08375, BAD_RS03325, and BAD_RS05655 may activate ATP-binding protein to participate in transportation. Compared with X2/X3, except that gene expression of BAD_RS05655 was downregulated, the remaining three ATP-binding proteins were upregulated (Table 1 and Figure 5). Therefore, high-polymerized XOS require highly expressed permease and ATP-binding protein to transport substrates into cells in *B. adolescentis*.

After entering the cell through cell membrane, XOS are degraded by endo-1,4-beta-xylanase (xylA) and β-xylosidase (xynB). In general, xylA randomly cleaves β-1,4 glycosidic bond of XOS, while xynB degrades XOS at the nonreducing end to release D-xylose [29]. Compared to X2/X3, the gene expressions of xynA (BAD_RS08020) and xynB (BAD_RS02270 and BAD_RS06360) in X5 treatment were upregulated (Table 2 and Figure 5). Both xylanase and xylosidase belong to glycoside hydrolase 43 family protein, for which the higher expression is conducive to the degradation of XOS [30]. In the present study, the gene expression related to transport and degradation of different polymerized XOS in *B. adolescentis* had a considerable difference, consistent with their functional association.

After XOS were degraded to D-xylose, D-xylose was isomerized to D-xylulose using xylose isomerase (xylA). Compared to the X2/X3, the expression of gene encoding xylose isomerase (BAD_RS02240) was not significantly different, while the content of D-xylulose (meta_85) was significantly increased in X5 treatment (Table 3 and Figure 5). Xylulose was further phosphorylated to xylulose-5-phosphate by xylulose kinase, but the xylulose kinase coding gene (BAD_RS06130) between the two treatment groups was not significantly different. Hereafter, xylulose 5-phosphate is converted to glyceraldehyde 3-phosphate using xylulose-5-phosphate phosphoketolase (XPPKT) [31, 32]. Compared to the X2/X3 treatment, the expression of gene encoding XPPKT (BAD_RS03665) was downregulated in the X5 treatment, but the difference was not significant. Glyceraldehyde 3-phosphate produces diphosphoglyceric acid under the action of glyceraldehyde-3-phosphate dehydrogenase (GAPDH). Diphosphoglyceric acid continues to generate

phosphoenolpyruvate using phosphoglycerate kinase (PGK). Compared with X2/X3, the expression of gene GAPDH (BAD_RS05735) and PGK (BAD_RS04470) was slightly downregulated in X5 treatment, but the difference was not significant. Phosphoenolpyruvate is converted to pyruvate after dephosphorylation (Figure 5). Metabolome analysis showed that phosphoenolpyruvate (meta_183) and pyruvate (meta_8) were downregulated in the X5 treatment group compared with X2/X3 (Table 3). The pyruvate is furtherly metabolized to different organic acids, such as lactic acid. The catabolic pathway of XOS is consistent with the pathway of *B. adolescentis* LMG10502 studied by Lagaert et al. [33], but it is different from the metabolic pathway of *B. longum*, which degrades XOS outside the cell by xylanase and then transports the degraded xylose into the cell for further metabolism [4].

4. Conclusions

From the present study, we can conclude that *low-polymerized XOS promoted the growth of B. adolescentis than the high-polymerized one*. When different polymerized XOS were used as a single carbon source, the related genes in annotated 51 metabolic pathways were significantly different, especially the ABC transporter pathway. Moreover, 192 differential metabolites were noted on MS2, and the mainly identified metabolites were organic acids. In summary, the expression of ABC transporter-related genes was significantly different during the process of different polymerized XOS transported into cells; however, the expression of most genes and metabolites related to XOS metabolism was not significantly different after entering the bifidus pathway, indicating the related proteins of ABC transport system played a key role on the process of *B. adolescentis* utilizing different polymerized XOS.

Data Availability

The data used to support the findings of this study are available from the corresponding author upon request.

Conflicts of Interest

All authors declare that they have no conflicts of interest to report.

Authors' Contributions

Di Yao designed the study. Mengna Wu carried out the preparation of XOS. Di Yao and Mengna Wu analyzed the DEGs and metabolites. Xiaoyu Wang performed qRT-PCR. Lei Xu conducted the data analysis. Di Yao, Mengna Wu, and Xiaoyu Wang wrote the final version of the manuscript. All authors read and approved the final version of the manuscript.

Acknowledgments

This study was supported by the Heilongjiang Natural Science Foundation Project (LH2019C049) and the Heilongjiang Significant Special Project of Engineering Science and Technology (2019ZX06B02). It was also supported by the Fund of the Scientific Research Starting Foundation for the Doctoral Program (no. XDB2017-12) and Innovative Talents Project (no. CXRC2017010), Heilongjiang Bayi Agricultural University.

Supplementary Materials

Supplementary Table 1: selected genes and primers for qRT-PCR. Supplementary Figure 1: HPLC analysis results of different polymerized XOS components after purification: A: xylobiose/xylotriose components; B: xylopentaose components. Supplementary Figure 2: change levels of global DEGs between X2/X3 and X5 treatment. Red dot: upregulated; green dot: downregulated; black dot: not DEGs. *s* (*Supplementary Materials*)

References

[1] R. D. Rolfe, "The role of probiotic cultures in the control of gastrointestinal health," *Journal of Nutrition*, vol. 130, no. 2, pp. 396S–402S, 2000.

[2] A. R. Lomax and P. C. Calder, "Prebiotics, immune function, infection and inflammation: a review of the evidence," *British Journal of Nutrition*, vol. 101, no. 5, pp. 633–658, 2009.

[3] C. E. Childs, H. Röytiö, E. Alhoniemi et al., "Xylo-oligosaccharides alone or in synbiotic combination with *Bifidobacterium animalis* subsp. lactis induce bifidogenesis and modulate markers of immune function in healthy adults: a double-blind, placebo-controlled, randomised, factorial cross-over study," *British Journal of Nutrition*, vol. 111, no. 11, pp. 1945–1956, 2014.

[4] L. A. M. van den Broek, S. W. A. Hinz, G. Beldman, J.-P. Vincken, and A. G. J. Voragen, "Bifidobacterium carbohydrases-their role in breakdown and synthesis of (potential) prebiotics," *Molecular Nutrition & Food Research*, vol. 52, no. 1, pp. 146–163, 2008.

[5] K. Pokusaeva, G. F. Fitzgerald, and D. van Sinderen, "Carbohydrate metabolism in bifidobacteria," *Genes & Nutrition*, vol. 6, no. 3, pp. 285–306, 2011.

[6] C.-K. Hsu, J.-W. Liao, Y.-C. Chung, C.-P. Hsieh, and Y.-C. Chan, "Xylooligosaccharides and fructooligosaccharides affect the intestinal microbiota and precancerous colonic lesion development in rats," *Journal of Nutrition*, vol. 134, no. 6, pp. 1523–1528, 2004.

[7] G. R. Gibson, H. M. Probert, J. V. Loo, R. A. Rastall, and M. B. Roberfroid, "Dietary modulation of the human colonic microbiota: updating the concept of prebiotics," *Nutrition Research Reviews*, vol. 17, no. 2, pp. 259–275, 2004.

[8] J. G. Yong and T. R. Klaenhammer, "Genetic mechanisms of prebiotic oligosaccharide metabolism in probiotic microbes," *Annual Review of Food Science and Technology*, vol. 6, no. 1, pp. 137–156, 2015.

[9] M. Okazaki, S. Fujikawa, and N. Matsumoto, "Effects of xylooligosaccharide on growth of bifidobacteria," *Nippon Eiyo Shokuryo Gakkaishi*, vol. 43, no. 6, pp. 395–401, 1990.

[10] A. Santos, M. San Mauro, and D. M. Díaz, "Prebiotics and their long-term influence on the microbial populations of the mouse bowel," *Food Microbiology*, vol. 23, no. 5, pp. 498–503, 2006.

[11] A. Amaretti, T. Bernardi, A. Leonardi, S. Raimondi, S. Zanoni, and M. Rossi, "Fermentation of xylo-oligosaccharides by

Bifidobacterium adolescentis DSMZ 18350: kinetics, metabolism, and β-xylosidase activities," *Applied Microbiology and Biotechnology*, vol. 97, no. 7, pp. 3109–3117, 2013.

[12] P. Bondue and V. Delcenserie, "Genome of Bifidobacteria and carbohydrate metabolism," *Korean Journal for Food Science of Animal Resources*, vol. 35, no. 1, pp. 1–9, 2015.

[13] M. S. Khoroshkin, S. A. Leyn, D. Van Sinderen, and D. A. Rodionov, "Transcriptional regulation of carbohydrate utilization pathways in the Bifidobacterium genus," *Frontiers in Microbiology*, vol. 7, no. 7, p. 120, 2016.

[14] S. Arboleya, F. Bottacini, M. O'Connell-Motherway et al., "Gene-trait matching across the *Bifidobacterium longum* pangenome reveals considerable diversity in carbohydrate catabolism among human infant strains," *BMC Genomics*, vol. 19, no. 1, p. 33, 2018.

[15] K. James, M. O. Connell Motherway, C. Penno, R. L. O. Brien, and D. V. Sinderen, "*Bifidobacterium breve* UCC2003 employs multiple transcriptional regulators to control metabolism of particular human milk oligosaccharides," *Applied and Environmental Microbiology*, vol. 84, no. 9, pp. 278-279, 2018.

[16] R. G. Crittenden and M. J. Playne, "Purification of food-grade oligosaccharides using immobilised cells of Zymomonas mobilis," *Applied Microbiology and Biotechnology*, vol. 58, no. 3, pp. 297–302, 2002.

[17] A. Rogowski, J. A. Briggs, J. C. Mortimer et al., "Correction: corrigendum: Glycan complexity dictates microbial resource allocation in the large intestine," *Nature Communications*, vol. 7, no. 1, p. 10705, 2016.

[18] O. Gilad, S. Jacobsen, B. Stuer-Lauridsen, M. B. Pedersen, C. Garrigues, and B. Svensson, "Combined transcriptome and proteome analysis of *Bifidobacterium animalis* subsp. lactis BB-12 grown on xylo-oligosaccharides and a model of their utilization," *Applied and Environmental Microbiology*, vol. 76, no. 21, pp. 7285–7291, 2010.

[19] J. Yang, Q. Tang, L. Xu, Z. Li, Y. Ma, and D. Yao, "Combining of transcriptome and metabolome analyses for understanding the utilization and metabolic pathways of Xylo-oligosaccharide inBifidobacterium adolescentisATCC 15703," *Food Sciences and Nutrition*, vol. 7, no. 11, pp. 3480–3493, 2019.

[20] K. J. Livak and T. D. Schmittgen, "Analysis of relative gene expression data using real-time quantitative PCR and the 2−ΔΔCT method," *Methods*, vol. 25, no. 4, pp. 402–408, 2001.

[21] C. G. Fraga, B. H. Clowers, R. J. Moore, and E. M. Zink, "Signature-discovery approach for sample matching of a nerve-agent precursor using liquid Chromatography–Mass spectrometry, XCMS, and chemometrics," *Analytical Chemistry*, vol. 82, no. 10, pp. 4165–4173, 2010.

[22] D. Kim, G. Pertea, C. Trapnell, H. Pimentel, R. Kelley, and S. L Salzberg, "TopHat2: accurate alignment of transcriptomes in the presence of insertions, deletions and gene fusions," *Genome Biology*, vol. 14, no. 4, p. R36, 2013.

[23] A. Moure, P. Gullón, H. Domínguez, and J. C. Parajó, "Advances in the manufacture, purification and applications of xylo-oligosaccharides as food additives and nutraceuticals," *Process Biochemistry*, vol. 41, no. 9, pp. 1913–1923, 2006.

[24] F. Turroni, C. Milani, S. Duranti, J. Mahony, D. van Sinderen, and M. Ventura, "Glycan utilization and cross-feeding activities by Bifidobacteria," *Trends in Microbiology*, vol. 26, no. 4, pp. 339–350, 2018.

[25] J. M. Andersen, R. Barrangou, M. A. Hachem et al., "Transcriptional analysis of oligosaccharide utilization by Bifidobacterium lactisBl-04," *BMC Genomics*, vol. 14, no. 1, p. 312, 2013.

[26] M. Ejby, F. Fredslund, J. M. Andersen et al., "An ATP binding cassette transporter mediates the uptake of α-(1,6)-linked dietary oligosaccharides in Bifidobacterium and correlates with competitive growth on these substrates," *Journal of Biological Chemistry*, vol. 291, no. 38, pp. 20220–20231, 2016.

[27] M. Ejby, A. Guskov, M. J. Pichler et al., "Two binding proteins of the ABC transporter that confers growth of Bifidobacterium animalis subsp. lactis ATCC27673 on β-mannan possess distinct manno-oligosaccharide-binding profiles," *Molecular Microbiology*, vol. 112, no. 1, pp. 114–130, 2019.

[28] K. Yoshida, R. Hirano, Y. Sakai et al., "Bifidobacterium response to lactulose ingestion in the gut relies on a solute-binding protein-dependent ABC transporter," *Communications Biology*, vol. 4, no. 1, p. 541, 2021.

[29] M. Kobayashi, Y. Kumagai, and Y. Yamamoto, "Identification of a key enzyme for the hydrolysis of β-(1⟶3)-xylosyl linkage in red alga dulse xylooligosaccharide from *Bifidobacterium adolescentis*," *Marine Drugs*, vol. 18, no. 3, p. 174, 2018.

[30] S. Fushinobu and M. Abou Hachem, "Structure and evolution of the bifidobacterial carbohydrate metabolism proteins and enzymes," *Biochemical Society Transactions*, vol. 49, no. 2, pp. 563–578, 2021.

[31] I. Iliev, T. Vasileva, V. Bivolarski, A. Momchilova, and I. Ivanova, "Metabolic profiling of xylooligosaccharides by lactobacilli," *Polymers*, vol. 12, no. 10, p. 2387, 2020.

[32] M. Jungersen, A. Wind, E. Johansen, J. Christensen, B. Stuer-Lauridsen, and D. Eskesen, "The science behind the probiotic strain *Bifidobacterium animalis* subsp. lactis BB-12," *Microorganisms*, vol. 2, no. 2, pp. 92–110, 2014.

[33] S. Lagaert, S. Van Campenhout, A. Pollet et al., "Recombinant expression and characterization of a reducing-end xylose-releasing exo-oligoxylanase from *Bifidobacterium adolescentis*," *Applied and Environmental Microbiology*, vol. 73, no. 16, pp. 5374–5377, 2007.